Published in final edited form as:
*Virology*. 2012 November 25; 433(2): 385–394. doi:10.1016/j.virol.2012.08.035.

# Murine skin and vaginal mucosa are similarly susceptible to infection by pseudovirions of different papillomavirus classifications and species

**Alessandra Handisurya**[a,b], **Patricia M. Day**[a], **Cynthia D. Thompson**[a], **Christopher B. Buck**[a], **Kihyuck Kwak**[c], **Richard B. S. Roden**[c], **Douglas R. Lowy**[a], and **John T. Schiller**[a,*]

[a]Laboratory of Cellular Oncology, Center for Cancer Research, National Cancer Institute, National Institutes of Health, Bethesda, MD 20892, USA

[b]Medical University of Vienna, Department of Dermatology, Division of Immunology, Allergy and Infectious Diseases, Vienna A-1090, Austria

[c]Department of Pathology, Johns Hopkins University, Baltimore, MD 21287, USA

## Abstract

Depending upon viral genotype, productive papillomavirus infection and disease display preferential tropism for cutaneous or mucosal stratified squamous epithelia, although the mechanisms are unclear. To investigate papillomavirus entry tropism, we used reporter pseudovirions based on various cutaneous and mucosal papillomavirus species, including the recently identified murine papillomavirus. Pseudovirus transduction of BALB/c mice was examined using an improved murine skin infection protocol and a previously developed cervicovaginal challenge model. In the skin, HPV5, HPV6, HPV16, BPV1 and MusPV1 pseudovirions preferentially transduced keratinocytes at sites of trauma, similar to the genital tract. Skin infection, visualized by *in vivo* imaging using a luciferase reporter gene, peaked between days 2–3 and rapidly diminished for all pseudovirion types. Murine cutaneous and genital tissues were similarily permissive for pseudovirions of HPV types 5,6,8,16,18,26,45,51,58 and animal papillomaviruses BPV1 and MusPV1, implying that papillomavirus' tissue and host tropism is governed primarily by post-entry regulatory events in the mouse.

### Keywords

papillomavirus; pseudovirions; murine model; skin infection; tissue tropism; murine papillomavirus; *in vivo* imaging

## Introduction

Papillomaviruses (PV) comprise a group of small, non-enveloped DNA viruses that infect humans and many other vertebrate species. To date, more than 180 genotypes have been characterized and classified into 29 genera (Bernard et al., 2010), based on the nucleotide sequence relatedness of the PV major capsid protein L1. Productive infection and induction of neoplasia is species-specific and PVs that affect humans (HPV) are clustered in five of these genera, namely alpha, beta, gamma, mu and nu. Additionally, HPVs can be designated as either a cutaneous or mucosal type based on the preferential productive lesion/papilloma

*Corresponding author: J. T. S., Laboratory of Cellular Oncology, Center for Cancer Research, National Cancer Institute, National Institutes of Health, 37 Convent Drive, Bethesda, MD 20892, USA, Phone: +1-301-594-2715, Fax: +1-301-480-5322, schillej@mail.nih.gov.

formation in stratified squamous epithelia of skin or mucosa, respectively. However, these designations represent infection preferences, rather than absolute requirements for infection of a specific anatomical area. For example, HPV 2, a common cause of verrucae vulgares on the skin, can also be detected in benign vulvar warts of children (Aguilera-Barrantes et al., 2007) and in oral lesions (de Villiers, 1989). HPV 8, which is responsible for the development of non-melanoma skin cancer in Epidermodysplasia verruciformis patients and possibly in non-genetically predisposed individuals (Gewirtzman et al., 2008), has been detected in some oropharyngeal tumors (Lindel et al., 2009). Conversely, mucosal HPVs can also infect skin sites. High-risk mucosal HPV types were detected in digital Bowen´s diseases and squamous cell cancers (SCC), some of these in association with concomitant or antecedent genital malignancies (Forslund et al., 2000; Kreuter et al., 2009). High-risk mucosal HPV 26 has been detected in a few cervical carcinomas, but recently has more often been found in SCC of the fingers and toes of individuals infected with HIV-1 (High et al., 2003; Kreuter et al., 2005; Handisurya et al., 2007).

Tissue tropism cannot be explained solely by the phylogeny of PV types. For instance, the mucosal HPV types 6 and 11, which share 85% sequence identity within their L1 genes, show differences in their predilection for specific sites. HPV 6 is more commonly found in anogenital warts than HPV 11, while HPV 11 is found more frequently in laryngeal papillomas. The closely related type HPV 13, which has 78% sequence identity to both HPV 6 and 11, causes focal epithelial hyperplasia of the oral cavity and has not been detected in either anogenital or laryngeal papillomas (Syrjanen, 2003). HPV 7 and 40, both sharing 87% L1 nucleotide sequence identity, also affect different anatomical sites. HPV 7 is responsible for Butcher´s warts, particularly on the hands of meat handlers, while HPV 40 causes mucosal papillomas of the anogenital and laryngeal tract. (Do you want to add a reference?) It is important to note that infection is often identified as a clinically apparent lesion, so apparent tropism may often correspond to sites at which papillomatous changes can be induced, with the possibility that sites of asymptomatic infection remain underappreciated.

The reasons for the observed tissue tropism are unclear, despite several attempts to clarify the factors responsible for preferential PV infection and/or induced neoplasia at specific sites. Characterization of the genetic elements that control tissue tropism has suggested that the long control (LCR) or upstream regulatory region serve to influence the tropism of HPV types (Steinberg et al., 1989). This region contains enhancer elements that show some tissue or cell type specificity and likely play a role in the initial expression of the viral genes after virus infection (Howley, 2007). Differences in the capacity of transcriptional activation have been shown for the LCR of cutaneous HPV 5 and mucosal HPV 16, using cell lines of different derivations (Mistry et al., 2007). Furthermore, prediction of transcription factor binding sites revealed that, while some binding sites are present in all LCRs, e.g. AP-1, other binding sites are restricted to certain genera or even HPV types (Garcia-Vallve et al., 2006). These differences in the LCR may singly, or in combination, have an impact on the preferential infection of distinct types of epithelia by the individual PV genotype.

Another factor in the determination of tissue tropism could be the interaction of the PV capsid proteins with host attachment factors. *In vivo*, attachment to negatively charged heparan sulfate proteoglycans (HSPG) on the basement membrane (BM) is regarded as the initial step leading to infection, at least for types examined until now: HPV 5, HPV 16, HPV 31 and HPV 45 (Johnson et al., 2009; Schiller et al., 2010). After undergoing a conformational change followed by furin cleavage of the L2 minor capsid protein, the L1 major capsid protein is thought to bind to a still undetermined secondary receptor on the cell surface, leading to internalization of the virus (Kines et al., 2009). It has been suggested that differences in the surface charge of PV L1 proteins may influence viral attachment, and modeling of the net surface charges has suggested that cutaneous HPV exclusively display

negatively charged L1 surfaces, whereas positively charged L1 surfaces were predominantly modeled for mucosal alpha-PV (Mistry et al., 2008). Whether these hypothetical differences affect infectious entry tropism *in vivo* is unclear. HSPGs do show great variability across individual cell types, due to differences in sulfation patterns and other chemical modifications of the heparin sulfate side chains, which are the target of initial PV binding (Turnbull et al., 2001). This heterogeneity might theoretically skew the binding of virions towards cells or the BM of cutaneous and/or mucosal origins. However, it is important to note that HSPGs are invariably negatively charged and would therefore be expected to interact with positively charged peptides on the virion surface.

To investigate whether the tissue specificity of cutaneous and mucosal PV types is determined at the level of infectious entry, from BM binding through establishment of the genome in the nucleus to initiate transcription, we have determined the *in vivo* infectivity of PV pseudovirions (PsV) concomitantly at a cutaneous and a mucosal site. Cutaneous exposure was achieved using an improved murine model for skin infection and mucosal exposure employed a previously published cervicovaginal challenge model of PV transmission (Roberts et al., 2007). The use of PsV allowed the delivery of an identical reporter plasmid (pseudogenome), thereby eliminating the potential confounding variability in gene expression for native PV genomes. Additionally, PsV infection can be readily and repeatedly quantified *in vivo* in an animal over an extended time course, using luciferase gene expression as a marker of infection. We included PsV of the recently identified mouse papillomavirus, Mus PV 1 (Ingle et al., 2011), to assess the possibility that infection tropism or kinetics might be influenced by a natural host versus a heterologous host species.

## Results

### PsV preparations of different PV types have variable particle to infectivity ratios in vitro

PsV representative of cutaneous (HPV 5, 8), low- (HPV 6, 44) and high-risk mucosal HPV types (HPV 16, 18, 26, 45, 51, 58), and two animal PV, bovine PV type 1 (BPV 1) and the recently identified murine PV, Mus PV 1, were generated by encapsidation of the reporter plasmid pCLucf, which contains a luciferase expression cassette (Johnson et al., 2009). In addition to luciferase, this reporter plasmid also expresses enhanced green fluorescent protein (GFP), which means the *in vitro* infectivity of PsV carrying pCLucf can be monitored by flow cytometric measurement of GFP expressing cells or luciferase. To evaluate the relative infectivity of cutaneous and mucosal PV types, the amount of encapsidated pCLucf reporter plasmid for various PsV stocks was calculated by quantitative PCR (qPCR) and compared to the GFP-transducing potential of the stock on a per cell basis of 293TT cells *in vitro*. Surprisingly, the observed particle to infectivity ratios were highly variable for different PV types (Table 1). The lowest mean ratios of 23, 37, 53 and 28 (i.e. most potent per particle infectivity) were observed for the high-risk mucosal HPV types 45, 58 and 26 and the new murine PV, Mus PV 1, respectively. The highest mean ratio of 4811 was obtained with preparations of cutaneous HPV 5. The ratios were similar among different preparations of the same PsV type (Table 1). The slight variabilities observed are likely due to minor differences in the passage number or physiological state of the producing cell line 293TT at time of PsV production. No correlation between the calculated ratios and the genera or tissue tropism of the PVs was evident. Furthermore, because empty capsids might compete with the transduction of the pseudogenome, we also determined the number of L1 capsids per $1\times10^9$ encapsidated pCLucf reporter plasmids. $1\times10^9$ reporter copies was chosen for this calculation because this number of PsV was used in subsequent *in vivo* infection studies. The range of the calculated ratios was between 1.4 to 5.51 present in the stock. No correlation was observed between reporter plasmid encapsidation efficiency and infectivity (Table 1).

## An improved murine skin challenge model allows efficient and consistent infection with PV PsV

We next established an efficient and reliable method for infection of murine skin that could be used to compare the relative *in vivo* infectivity of different PsV preparations in the skin and cervicovaginal tract. PsV encapsidating the luciferase reporter plasmid pCLucf were employed in all experiments to enable readout by *in vivo* imaging analysis, as this method allows sequential *in situ* quantitative assessment of infection in the same living animal. An essential feature of the recently developed murine model for cervicovaginal infection of PsV (Roberts et al., 2007) was the deliberate disruption of the vaginal epithelium, as intact epithelia were found to be resistant to PV infection. However, deliberate disruption was not used in the previously reported skin challenge model (Gambhira et al., 2007; Alphs et al., 2008). We found that skin disruption with a hand rotary device with an attached felt wheel followed by pipette delivery of PsV solutions and scoring the liquid into the pre-scarified area allowed for the most efficient and reproducible infection. This procedure was more consistent and robust than the previous reported method of applying the PsV to freshly shaved skin (Gambhira et al., 2007; Alphs et al., 2008). Repeated evaluations for consistency of our new method using identical amounts of the same PsV preparation (e.g. corresponding to $1\times10^9$ reporter plasmid copies in Mus PV 1 PsV) over a time period of 6 months in 15 animals from different animal batches and of different ages gave similar luminescence signals in all animals, with average radiance values ranging from $2.1\times10^4$ to $2.5\times10^5$ p/s/cm$^2$/sr (mean average radiance $8.3\times10^4$ p/s/cm$^2$/sr). This improved abrasive technique with the hand rotary device enabled directed and evenly distributed removal of the epidermis layer by layer until the BM is exposed and evolved as the fastest and easiest method for testing large numbers of mice. Furthermore, compared to the second best method of skin disruption (in our hands), namely manual scarification using a razor blade, abrasion with the hand rotary device resulted in 1 log higher luminescence signals, as determined by side-by-side comparison using the same amount and stock of PsV, and was less traumatic for the animals. To initiate infection, PsV solutions were delivered onto the pre-scarified area by pipette delivery and scored into the skin. Similar to the cottontail rabbit PV (CRPV) model (Cladel et al., 2008), inoculation with PsV three days after scarification gave the most consistent results, whereas inoculation immediately after scarification proved inefficient. For example, when $1\times10^9$ of Mus PV 1 reporter were used, inoculation performed immediately after scarification resulted in luminescence signals, that, if positive at all, were almost 2 logs lower compared to inoculation performed three days after scarification using the same stock and amount of PsV (e.g. mean $1.4\times10^3$ p/s/cm$^2$/sr versus mean $7.7\times10^4$ p/s/cm$^2$/sr, respectively).

Figure 1 shows visualization of murine skin infection three days after PsV inoculation. Imaging of mice prior to intraperitoneal administration of the substrate luciferin consistently revealed no luminescence signal (Fig. 1A and 1C). On the third day after inoculation with $1\times10^9$ copies of pCLucf pseudogenome, a positive signal was readily detected as soon as three minutes after luciferin administration. The luminescent signal strength steadily rose until reaching a plateau at 15–20 minutes (data not shown). Figure 1B shows *in vivo* imaging of mice using PsV based on the recently identified Mus PV 1 (Ingle et al., 2011) ten minutes after administration of luciferin. Luminescence signals of control mice that had received phosphate-buffered saline (PBS) instead of PsV preparations remained undetectable at any timepoint after substrate administration (Fig. 1D).

## PsV of diverse origin infect murine epidermal keratinocytes

To determine the cellular distribution of PsV infection in skin, mice were simultaneously challenged with PsV preparations encapsidating either the reporter plasmid pCLucf or pNaMB. The use of the luciferase plasmid facilitated precise excision of the inoculated area

by luminometric-imaging immediately prior to necropsy. The pNaMB plasmid, encoding a "tailless" non-signaling fragment of human CD4, enabled detection and localization of the infected cells within the biopsied material, by immunofluorescent staining and confocal microscopy. Human CD4 was selected as a marker for PsV infection because of its distinctive cell surface localization and the availability of reliable commercial antibodies suitable for its detection by immunohistochemistry. Efforts to microscopically detect the expressed luciferase protein did not yield consistent and satisfactory results.

Figure 2 shows immunofluorescent confocal microscopy analyses of murine skin three days after challenge with representatives of human and animal PsV. HPV 5 (Fig. 2A) and HPV 16 (Fig. 2B) were chosen as representatives of cutaneous and mucosal HPV types, respectively. Mus PV 1 (Fig. 2C and 2F) was chosen because it represents a PV for which the mouse is the natural host, while BPV 1 (Fig. 2D) represents an animal PV for which the mouse is a heterologous host. Co-staining for CD49f (integrin alpha-6), which is highly expressed in basal keratinocytes especially along the basal aspect of these cells (Stepp et al., 1990), was concomitantly detected to enable localization of PsV infected cells relative to these cells. For every PV type investigated, virally-infected cells were distributed within the epithelium of the skin overlying the BM. As expected, CD4 expression was clearly associated with the cell surface of cells with keratinocytic morphology. No differences in the pattern of infected cells were noted among the individual PsV types. Skin tissue sections from mice mock-infected with PBS served as controls to determine specificity (Fig. 2E). These tissues lacked specific staining with anti-human CD4, but readily showed staining of the basal keratinocytes with anti-CD49f. Staining of murine vaginal tissues infected with Mus PV 1 PsV (Fig. 2F) revealed staining of epithelial cells in a distribution similar to PsV of other PV types as reported previously (Roberts et al., 2007), demonstrating that Mus PV 1 PsV are able to infect vaginal tissues. Vaginal tracts of mice that received PBS again served as specificity controls and did not reveal anti-CD4 staining (data not shown).

## Skin infection peaks at day 2–3 for cutaneous and mucosal types

To determine the dynamics of skin infection, *in vivo* imaging analysis was employed in mice challenged with PsV of various PV types, each expressing $1\times10^9$ copies of the luciferase-reporter plasmid. Luminescence was measured each day for a total of 10 days. At each timepoint, luminescence was measured prior to administration of the substrate to ensure that there were no residual signals from the preceding day. The time course of *in vivo* skin infection of representative PsV types, HPV 5, HPV 6, HPV 16, BPV 1 and Mus PV 1, are shown in Figure 3. For all PsV types investigated, luminescence signals were detectable one day after infection, showed a sharp increase in intensity until a peak on either day two or day three, and rapidly declined thereafter. A notable exception to this pattern was that Mus PV 1 reproducibly exhibited a slower decline in signal, dropping to below 5% of maximum value only after 7 days. For all PsV types tested, the luminescence signals remained undetectable after they returned to background levels.

## PsV of cutaneous and mucosal human and animal PV types similarily infect murine tissues of cutaneous and mucosal-genital origin

We next compared the efficiency of cutaneous versus mucosal infectivity of different PsV types. To ensure comparability of *in vivo* infectivity, PsV preparations of the different PV types, each containing $1\times10^9$ luciferase reporter plasmid copies, were used as above for each inoculation, and the same mouse was concomitantly infected at both the skin on the back and the cervicovaginal tract. The luciferin substrate was delivered by intraperitoneal administration to allow similar distribution of the substrate to the two sites within the same mouse. Luminescence was detected on day 2 and 3 after infection, based on the previously determined maxima in luminescence signals for the skin and the reported peak for

cervicovaginal tissues (Roberts et al., 2007; Day et al., 2010). Figure 4 shows representatives of cutaneous and mucosal low- and high-risk HPV types as well as the two animal PV types.

Genital luminescence tended to be higher on day 2 than day 3, whereas the opposite was true for skin sites. However, HPV 5 and 8, which are closely related cutaneous types, infected skin and cervicovaginal tissues and exhibited higher levels at day 2 at both sites (data shown for HPV 5). The luminescent intensity for HPV 6, a representative of low-risk mucosal HPV, was initially higher in the genital tract compared to the cutaneous site, by day three the luminescence signal peaked for the skin, whereas the signal had sharply declined in the cervicovaginal tract. Therefore, despite differences in the kinetics of infection, the overall infectivity of both tissues was approximately equal. The low-risk mucosal HPV 44 behaved similarly to HPV 6 (data not shown).

PsV of several high-risk mucosal HPV types were generated and studied, including HPV 16, 18, 26, 45, 51, and 58. Two trends emerged from this analysis. For HPV type 16, 18, and 45, overall infectivity appeared to be equal between the infected tissue types, similar to the results observed with low-risk mucosal HPV. However, HPV 26, 51 and HPV 58 (data for HPV 51 and 58 not shown) exhibited somewhat greater infection of the skin on day two as well as on day three, compared to genital tissues. However, these differences were not significant.

PsV of representative animal PV, Mus PV 1 and BPV 1, similarly revealed slight superiority in the efficiency of cutaneous infection compared to cervicovaginal infection. On a per pseudogenome basis, Mus PV 1 was one of the more efficient PsV at infecting the mouse skin and vaginal tract, but not more efficient than HPV 26. Thus, it does not appear that species-restricted interactions play a major role in early events of PV infection.

## Discussion

In this study, we use PV pseudovirus technology to address the entry tropism of different PV types in the mouse. Although our previous studies had demonstrated infection of the cervicovaginal tissue with HPV 5, a cutaneous type, this infection was substantially weaker than that of HPV 16 and HPV 31 shown in the same study (Johnson et al., 2009). Therefore, we considered the possibility that some measure of tropism could be determined at the level of initial capsid interaction with the BM or viral entry into target keratinocytes.

Results from the murine model for cervicovaginal infection (Roberts et al., 2007) showed that disruption of the epithelium, which allows access and binding of the virions to the BM, appears to be necessary for initiation of PV infection of the cervicovaginal tract *in vivo*. To establish an improved model for murine skin infection, several methods of physical and/or chemical cutaneous disruption were assessed. These included “tape-stripping”, abrasion with sandpaper, scarification with razor blades, placement of a microneedle patch, pre-hydration of skin with water or ethanol to induce swelling of the keratinocytes, or application of Nonoxynol-9, the non-ionic membrane-active surfactant that is used to disrupt the epithelium in the cervicovaginal challenge model. In our hands, scarification with a hand rotary device with an attached felt wheel emerged as the most consistent, robust and reproducible method for *in vivo* infection of murine skin, resulting in substantially higher luminescence signals compared to other methods tested (data not shown). Employing this improved model of cutaneous challenge, we found that skin and mucosal tissues are both susceptible to *in vivo* infection by PsV of different cutaneous and mucosal PV types and species. No major differences were observed in the overall efficiency of infection among different human and animal PsV types. With all analyzed types, the infected keratinocytes

within the epithelium were observed in a linear array, highly suggestive that infected keratinocytes migrated from the basal layers towards the surface during the differentiation process. No indication of infection of other cell types was observed in either skin or genital sites for any of the PV types examined.

Although subtle differences in the kinetics of PsV infection of skin and of genital tissues were observed, the biological relevance of this observation is unclear. It is more plausible that these differences are attributable to the methods of infection. For cervicovaginal infection, inoculation with PsV was performed four hours after chemical disruption of the epithelium with the anionic detergent, Nonoxynol-9. Histologic analysis revealed that at that time point the genital epithelium is partially ablated, allowing access of PsV to the BM. In the skin challenge model, infection was initiated three days after physical disruption of the epithelial layers. The resultant scab, present on the previously scarified area, overlying the denuded epithelium, may delay diffusion of the PsV to the BM. Furthermore, in contrast to the genital tract, inoculation performed immediately after scarification did not result in reliable infection. It is conceivable that this is due to the PsV inoculum becoming entrained in the vigorous serum exudates that occurs immediately after skin abrasion and is unable to efficiently reach the BM. Alternatively, perhaps the induction of the scab after cutaneous wounding retards migration of the keratinocytes over the exposed BM relative to their migration rate in wounded cervcovaginal epithelium. Prolonged exposure of the capsids on the BM before contacting the keratinocytes might make them more susceptible to engulfment by monocytes and neutrophils that would be expected to also migrate into the sites of wounding. However, immunofluorescent staining of skin tissues three days after infection did not indicate infection of cell types other than keratinocytes. If the PsV do interact with phagocytic cells in this setting, it is likely that they are routed down a degradative rather than an infectious pathway.

When comparing different PsV types within the skin model, some differences in the kinetics of infection were observed. Analysis of HPV 5 PsV revealed short-lasting expression with a rapid decline, which became undetectable after only three days, even on the skin, which is thought to be the “appropriate” target site. In contrast, luminescence signals of high-risk mucosal HPV 16 were measurable for a period of up to six days, although the peak signal was similar for the two PsV types (Fig. 3). This difference in the duration of expression is puzzling, since the same luciferase pseudogenome was transduced and no viral genes were expressed. Perhaps infection is simply more asynchronous for HPV 16.

The recently identified murine PV emerged as an interesting new PV type. Mus PV 1 PsV showed a prolonged and very intense expression after infection of the skin. Whether this characteristic is due to factors involved in homologous infection or due to other virus-specific factors remains unclear. Further investigation to determine if this PV type is a superior vector for (trans)cutaneous vaccination strategies is warranted. Another interesting trend was observed with the high-risk mucosal types HPV 26 and HPV 58. These types seem to more efficiently infect cutaneous tissues. This observation is consistent with the finding that these types are often detected in the skin of fingers and toes of immunocompromised individuals. Why these types may be more amenable to infection of cutaneous epithelia remains to be elucidated.

Although the same number of reporter plasmid copies was used in all the *in vivo* experiments, the absolute numbers of average radiance varied between the individual experiments. The exact reasons for this observed phenomenon are difficult to decipher, but possible explanations include the fact that mice used for different experiments varied in age and batch, variabilities between readings with the IVIS on different days may have occured, and different PsV stocks were used in different experiments. However, *in vitro* titration on

293TT cells was broadly predictive for *in vivo* infectivity, although these cells are derived from a multiply-transformed human embryonic kidney cell line, that would appear to be of limited biological relevance to *in vivo* PV infection.

As PsV-based studies are capable of addressing the early events in the PV lifecycle, our results imply that differences in the availability of viral receptors, endosome escape, or genome trafficking to the nucleus do not account for the species specificity or preferential infection and neoplastic transformation of specific anatomical sites by PV. Previous studies have demonstrated that PV virus-like particles or native virions of BPV 1 can bind to a variety of cultured cell lines derived from various organs and animal species, implying a broad distribution of a PV receptor(s) involved in attachment (Roden et al., 1994; Volpers et al., 1995; Müller et al., 1995). However, the relevance of these observations to *in vivo* infection is unclear, given the differences in early events of infection *in vitro* and *in vivo* (Kines et al., 2009). Of more relevance, homologous (CRPV capsid/CRPV genome) and chimeric (HPV 16 capsid/CRPV genome) PV particles can successfully infect rabbit cutaneous tissues (Mejia et al., 2006). However, this assay has only a limited ability to quantify the extent of infection. The results described herein provide the strongest support to date for the notion that diverse PV types share common mechanisms for the early events of infection in mucosal and squamous epithelia, implying that downstream post-entry events are responsible for the PV species and tissue tropism. These may include qualitative and quantitative differences in the replication capacity of the viral genomes of PV types in cells of different origins or the availability of cellular factors determining viral gene expression. Clearly, further investigations on the post-entry molecular determinants are warranted to understand PV tissue tropism.

## Methods

### PsV production

PsV of cutaneous and mucosal HPV as well as animal PV were produced according to the protocol published on the laboratory website (http://www.ncbi.nlm.nih.gov/pubmed/18228512). Briefly 293TT cells, derived from a human embryonic kidney cell line and modified to express high levels of SV40 Large T antigen, were co-transfected with plasmid vectors expressing the PV major and minor capsid proteins, together with a reporter gene plasmid. Assembled particles encompassing the reporter gene were purified by Optiprep gradient centrifugation.

Nucleotide maps of the plasmid vectors for the different PV types, including the new murine PV, are available on the laboratory website. For generation of Mus PV 1 PsV, a bicistronic mammalian expression plasmid encoding the L1 and L2 proteins was created by synthetic codon-modification of the capsid protein open reading frames using a previously-reported algorithm (http://www.ncbi.nlm.nih.gov/pubmed/15051381) also available on our laboratory website. The major and minor capsid proteins of HPV types 8, 44, and 51 were codon-optimized (Kondo et al., 2009) and engineered into the double expression vector pVITRO1-neo-mcs (InvivoGen).

The pNaMB reporter gene plasmid was generated by transferring a C-truncated human CD4 open reading frame from pMACS-IRES-CD4 (Miltenyi Biotec Inc.) into pSU-5697 (Buck et al., 2004). The pCLucf plasmid has been described previously (Johnson et al., 2009). Nucleotide maps of the reporter gene vectors for human CD4 (pNaMB) and luciferase (pCLucf) are posted on the laboratory website.

293TT cells were maintained and grown in Dulbecco´s modified Eagle´s medium supplemented with 10% fetal bovine serum.

### Characterization and quantification of PsV preparations

Purified PsV preparations were characterized for their infectivity, their amount of major capsid protein L1 and encapsidated DNA, and for their reporter plasmid copy numbers.

Briefly, infectious titers of purified PsV preparations were determined by infecting 293TT cells with PsV containing pCLucf and measuring the number of GFP-positive cells by flow cytometric analysis 48 hours after infection (Kines et al., 2009). Titers are given in infectious units per milliliter (IU/ml).

The L1 content of the PsV preparations was quantified by sodium-dodecyl sulfate-polyacrylamide gel electrophoresis of purified PsV preparations followed by staining with SYPRO® Ruby (Molecular Probes, Life Technologies) according to the manufacturer´s protocol.

Encapsidated DNA contents of PsV preparations were determined by electrophoresis analysis on agarose gels after release of DNA from the L1/L2 capsids by proteinase K treatment (Johnson et al., 2009).

Reporter plasmid copy numbers were determined from encapsidated DNA, previously extracted from purified PsV preparations (protocol available on the laboratory website). After extraction DNA was subsequently analyzed by qPCR using the DyNAmo™ SYBR® Green qPCR Kit (Thermo Fisher Scientific Inc.) according to the manufacturer´s instructions using primers specific for GFP. The sequences for primers for GFP are as follows: forward primer 5´-GACTTCAAGGAGGACGGCAAC-3´, reverse primer 5´-GGTGTTCTGCTGGTAGTGGTCG-3´. The copy numbers were calculated using known amounts of pCLucf plasmids as standards and the ratio of reporter plasmid copy numbers to infectious units determined.

The determination of the ratio of capsids per reporter plasmid was made based on the calculation of 30,000 capsids per pg of L1, and the ratio was normalized to $1\times10^9$ reporter plasmid copies.

### Murine models of cutaneous and cervicovaginal PsV infection

Female BALB/cAnNCr mice of 6–8 weeks of age were obtained from the National Institutes of Health. Housing and handling were performed in accordance with their guidelines and experimental protocols were approved by the National Cancer Institute’s Animal Care and Use Committee.

For cutaneous PsV infection, the dorsal hair of the mice was removed three days prior to infection, first using an electric clipper followed by application of Nair (Church & Dwight Co., Inc) depilatory cream for 20 seconds. In order to remove the uppermost layers of the epidermis an area of 2×1.5 cm on the skin on the back was carefully scarified using a hand rotary device with an attached felt wheel (Dremel 300 series). After three days, infection was performed by pipetting the PsV solution in a total volume of 20 µl in PBS onto the previously scarified site followed by gently scoring the liquid into the skin using a 26 Gauge 3/8" needle without removal of the scab.

Cervicovaginal infection was performed according to a previously published protocol (Roberts et al., 2007). Briefly, mice received progesterone (3 mg Depo-Provera dissolved in 100 µl sterile PBS) subcutaneously on day −4 in order to potentiate susceptibility for infection. On day 0 the genital mucosa was disrupted by Nonoxynol-9 (Conceptrol, Mc Neil Pharmaceutical Inc.) treatment four hours prior to instillation of the PsV solution (total volume of 20 µl, dissolved in 4% carboxymethylcellulose (CMC)) into the vaginal vault.

### In vivo analysis of PsV infection

Determination of the luciferase activity in PV PsV-infected tissues represents a standard readout for infectivity, and expression of luciferase activity was measured using an *in vivo* luminescence imager. All PsV preparations were used in an amount of $1\times10^9$ reporter plasmid copy numbers, as determined by qPCR, for every infection regardless of tissue site. Readout was performed on the indicated days post infection by intraperitoneal injection of 100 µl of *D*-Luciferin Potassium Salt (15 mg/ml, diluted in Dulbecco´s modified Eagle´s medium) (Caliper Life Sciences) and imaging (ventral and dorsal view) using a IVIS 100 (Caliper Life Sciences) ten minutes after administration of the substrate with medium binning and 60 seconds exposure. Images were analyzed and the average radiance (given in p/s/cm2/sr) within the region of interest was determined with the Living Image 3.0 software (Caliper Life Sciences). Data are representative of five mice per group, and experiments were performed in duplicate. Statistical analysis was performed using the GraphPad Prism Software.

### Harvest of tissue samples

For immunofluorescent imaging studies, mice were infected with a mixture of PsV encapsidating either pCLucf or pNaMB according to the established protocol for skin or cervicovaginal infection. For skin specimens, imaging with IVIS 100 was performed three days post infection after intraperitoneal administration of *D*-Luciferin Potassium Salt to facilitate retrieval of the exact localization of the previously infected sites. Mice were then euthanized by $CO_2$ inhalation and skin necropsies were taken from the previously marked sites. To verify proper removal, biopsies were read again in the IVIS 100 and positive samples were subsequently snap frozen in Tissue-Tek OCT Compound freezing medium (Sakura Finetek).

For processing of the genital tract specimens, the entire genital vault was dissected after euthanization on day two post infection and snap frozen in Tissue-Tek OCT Compound freezing medium.

All tissue samples were stored at −80°C until further analysis.

### Immunofluorescent staining

Tissue sections were cut at 6 µm thickness, mounted on Superfrost Plus Microscope Slides (Fisher Scientific) and fixed by incubation in 100% ethanol for 10 min at −20°C. Nonspecific binding sites were blocked with 10% donkey serum (Jackson ImmunoResearch Laboratories Inc.) in PBS with 0.1% Brij 58 for 30 minutes at room temperature. A rat monoclonal antibody recognizing human CD4 (LifeSpan BioSciences Inc.) was used at a dilution of 1:200 and sections were incubated for 1 hour at 37°C. Detection was perfomed with Alexa Fluor 488-conjugated donkey anti-rat secondary antibody (Invitrogen, Life Technologies) diluted 1:1000. To visualize basal keratinocytes sections were co-stained with a phycoerythrin-labelled anti-CD49f antibody (integrin alpha 6, BD Pharmingen) for 1 hour at 37°C. Following staining, sections were mounted with ProLong® Gold antifade reagent containing DAPI (Molecular Probes, Life Technologies) to visualize nuclei.

All microscopy analysis was performed on a Zeiss LSM 510 UV system. Images were collated in Adobe Photoshop and color levels were adjusted uniformly across experiments before conversion to tiff format.

## Acknowledgments

This research was supported by the Intramural Research Program of the National Institutes of Health, National Cancer Institute, Center for Cancer Research and the Austrian Science Fund FWF (Erwin Schroedinger Fellowship project no.: J3012-B13 to AH) and Public Health Service grants CA133749, CA118790 and P50 CA098252.

## References

Aguilera-Barrantes I, Magro C, Nuovo GJ. Verruca vulgaris of the vulva in children and adults: a nonvenereal type of vulvar wart. Am J Surg Pathol. 2007; 31(4):529–535. [PubMed: 17414099]

Alphs HH, Gambhira R, Karanam B, Roberts JN, Jagu S, Schiller JT, Zeng W, Jackson DC, Roden RB. Protection against heterologous human papillomavirus challenge by a synthetic lipopeptide vaccine containing a broadly cross-neutralizing epitope of L2. Proc Natl Acad Sci U S A. 2008; 105(15):5850–5855. [PubMed: 18413606]

Bernard HU, Burk RD, Chen Z, van Doorslaer K, Hausen H, de Villiers EM. Classification of papillomaviruses (PVs) based on 189 PV types and proposal of taxonomic amendments. Virology. 2010; 401(1):70–79. [PubMed: 20206957]

Buck CB, Pastrana DV, Lowy DR, Schiller JT. Efficient intracellular assembly of papillomaviral vectors. J Virol. 2004; 78(2):751–757. [PubMed: 14694107]

Cladel NM, Hu J, Balogh K, Mejia A, Christensen ND. Wounding prior to challenge substantially improves infectivity of cottontail rabbit papillomavirus and allows for standardization of infection. J Virol Methods. 2008; 148(1–2):34–39. [PubMed: 18061687]

Day PM, Kines RC, Thompson CD, Jagu S, Roden RB, Lowy DR, Schiller JT. In vivo mechanisms of vaccine-induced protection against HPV infection. Cell Host Microbe. 2010; 8(3):260–270. [PubMed: 20833377]

de Villiers EM. Heterogeneity of the human papillomavirus group. J Virol. 1989; 63(11):4898–4903. [PubMed: 2552162]

Forslund O, Nordin P, Hansson BG. Mucosal human papillomavirus types in squamous cell carcinomas of the uterine cervix and subsequently on fingers. Br J Dermatol. 2000; 142(6):1148–1153. [PubMed: 10848738]

Gambhira R, Karanam B, Jagu S, Roberts JN, Buck CB, Bossis I, Alphs H, Culp T, Christensen ND, Roden RB. A protective and broadly cross-neutralizing epitope of human papillomavirus L2. J Virol. 2007; 81(24):13927–13931. [PubMed: 17928339]

García-Vallvé S, Iglesias-Rozas JR, Alonso A, Bravo IG. Different papillomaviruses have different repertoires of transcription factor binding sites: convergence and divergence in the upstream regulatory region. BMC Evol Biol. 2006; 6:20. [PubMed: 16526953]

Gewirtzman A, Bartlett B, Tyring S. Epidermodysplasia verruciformis and human papilloma virus. Curr Opin Infect Dis. 2008; 21(2):141–146. [PubMed: 18317036]

Handisurya A, Rieger A, Bankier A, Koller A, Salat A, Stingl G, Kirnbauer R. Human papillomavirus type 26 infection causing multiple invasive squamous cell carcinomas of the fingernails in an AIDS patient under highly active antiretroviral therapy. Br J Dermatol. 2007; 157(4):788–794. [PubMed: 17634082]

High WA, Tyring SK, Taylor RS. Rapidly enlarging growth of the proximal nail fold. Dermatol Surg. 2003; 29(9):984–986. [PubMed: 12930348]

Howley, PM.; Lowy, DR. Papillomavirus. In: Knipe, DM.; Howley, PM., editors. Fields Virology. Philadelphia: Lippincott Williams and Wilkins; 2007. p. 2299-2354.

Ingle A, Ghim S, Joh J, Chepkoech I, Bennett Jenson A, Sundberg JP. Novel laboratory mouse papillomavirus (MusPV) infection. Vet Pathol. 2011; 48(2):500–505. [PubMed: 20685915]

Johnson KM, Kines RC, Roberts JN, Lowy DR, Schiller JT, Day PM. Role of heparan sulfate in attachment to and infection of the murine female genital tract by human papillomavirus. J Virol. 2009; 83(5):2067–2074. [PubMed: 19073722]

Kines RC, Thompson CD, Lowy DR, Schiller JT, Day PM. The initial steps leading to papillomavirus infection occur on the basement membrane prior to cell surface binding. Proc Natl Acad Sci U S A. 2009; 106(48):20458–20463. [PubMed: 19920181]

Kondo K, Ishii Y, Mori S, Shimabukuro S, Yoshikawa H, Kanda T. Nuclear location of minor capsid protein L2 is required for expression of a reporter plasmid packaged in HPV51 pseudovirions. Virology. 2009; 394(2):259–265. [PubMed: 19766281]

Kreuter A, Brockmeyer NH, Pfister H, Altmeyer P, Wieland U. Competence Network HIV/AIDS. Human papillomavirus type 26-associated periungual squamous cell carcinoma in situ in a HIV-infected patient with concomitant penile and anal intraepithelial neoplasia. J Am Acad Dermatol. 2005; 53(4):737–739. [PubMed: 16198810]

Kreuter A, Gambichler T, Pfister H, Wieland U. Diversity of human papillomavirus types in periungual squamous cell carcinoma. Br J Dermatol. 2009; 161(6):1262–1269. [PubMed: 19663878]

Lindel K, Helmke B, Simon C, Weber KJ, Debus J, de Villiers EM. Cutaneous human papillomavirus in head and neck squamous cell carcinomas. Cancer Invest. 2009; 27(7):781–787. [PubMed: 19513898]

Mejia AF, Culp TD, Cladel NM, Balogh KK, Budgeon LR, Buck CB, Christensen ND. Preclinical model to test human papillomavirus virus (HPV) capsid vaccines in vivo using infectious HPV/cottontail rabbit papillomavirus chimeric papillomavirus particles. J Virol. 2006; 80(24):12393–12397. [PubMed: 17005666]

Mistry N, Simonsson M, Evander M. Transcriptional activation of the human papillomavirus type 5 and 16 long control region in cells from cutaneous and mucosal origin. Virol J. 2007; 4:27. [PubMed: 17352804]

Mistry N, Wibom C, Evander M. Cutaneous and mucosal human papillomaviruses differ in net surface charge, potential impact on tropism. Virol J. 2008; 5:118. [PubMed: 18854037]

Müller M, Gissmann L, Cristiano RJ, Sun XY, Frazer IH, Jenson AB, Alonso A, Zentgraf H, Zhou J. Papillomavirus capsid binding and uptake by cells from different tissues and species. J Virol. 1995; 69(2):948–954. [PubMed: 7815562]

Roberts JN, Buck CB, Thompson CD, Kines R, Bernardo M, Choyke PL, Lowy DR, Schiller JT. Genital transmission of HPV in a mouse model is potentiated by nonoxynol-9 and inhibited by carrageenan. Nat Med. 2007; 13(7):857–861. [PubMed: 17603495]

Roden RB, Kirnbauer R, Jenson AB, Lowy DR, Schiller JT. Interaction of papillomaviruses with the cell surface. J Virol. 1994; 68(11):7260–7266. [PubMed: 7933109]

Schiller JT, Day PM, Kines RC. Current understanding of the mechanism of HPV infection. Gynecol Oncol. 2010; 118(1 Suppl):S12–S17. [PubMed: 20494219]

Steinberg BM, Auborn KJ, Brandsma JL, Taichman LB. Tissue site-specific enhancer function of the upstream regulatory region of human papillomavirus type 11 in cultured keratinocytes. J Virol. 1989; 63(2):957–960. [PubMed: 2536117]

Stepp MA, Spurr-Michaud S, Tisdale A, Elwell J, Gipson IK. Alpha 6 beta 4 integrin heterodimer is a component of hemidesmosomes. Proc Natl Acad Sci U S A. 1990; 87(22):8970–8974. [PubMed: 2247472]

Syrjanen S. Human papillomavirus infections and oral tumors. Med Microbiol Immunol. 2003; 192(3): 123–128. [PubMed: 12920585]

Turnbull J, Powell A, Guimond S. Heparan sulfate: decoding a dynamic multifunctional cell regulator. Trends Cell Biol. 2001; 11(2):75–82. [PubMed: 11166215]

Volpers C, Unckell F, Schirmacher P, Streeck RE, Sapp M. Binding and internalization of human papillomavirus type 33 virus-like particles by eukaryotic cells. J Virol. 1995; 69(6):3258–3264. [PubMed: 7745672]

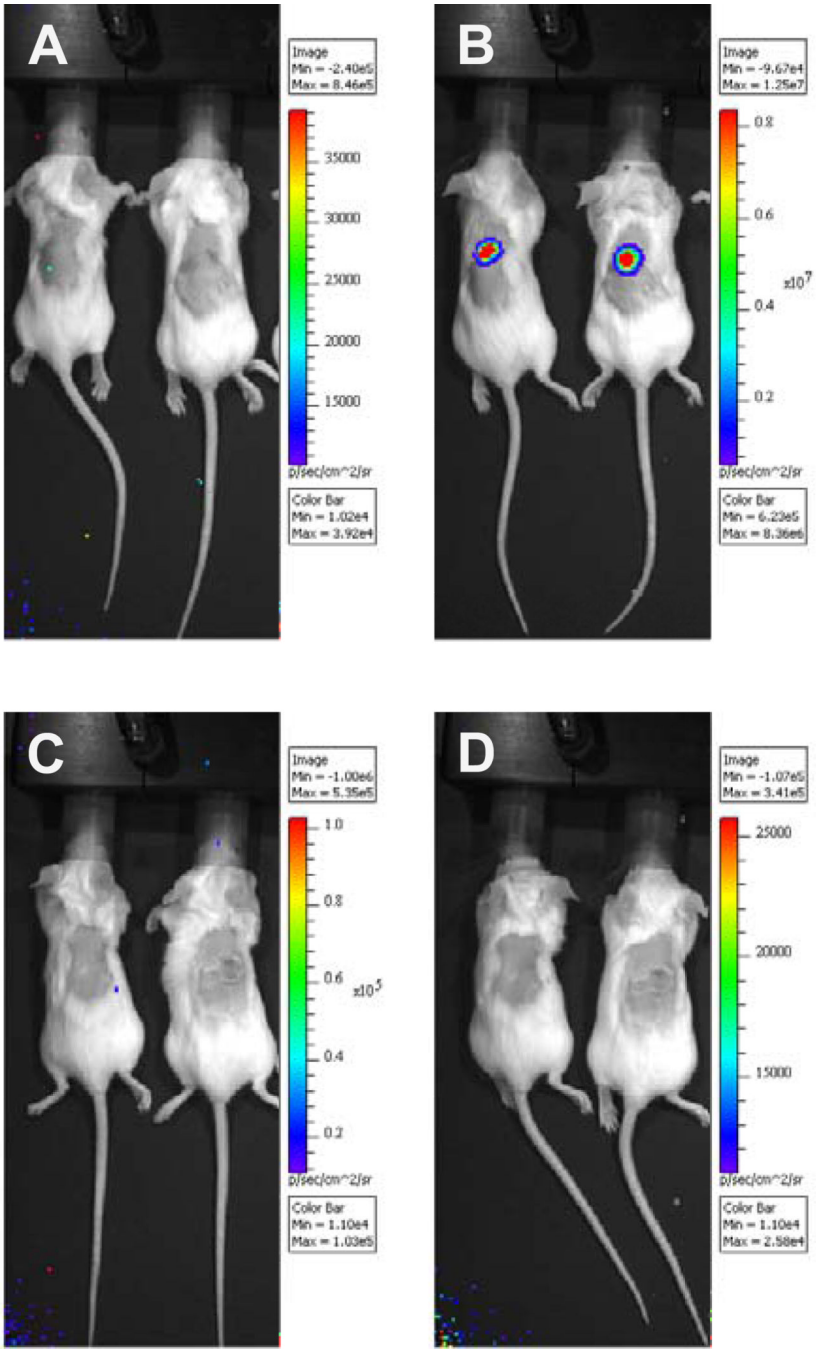


**Fig. 1.**

*In vivo* imaging of BALB/c mice three days after skin challenge. A luciferase expression plasmid was packaged into pseudovirions composed of the capsid proteins of the new mouse papillomavirus Mus PV 1. Mice were challenged cutaneously with a pseudovirus inoculum containing $1\times10^9$ copies of luciferase reporter plasmid (pseudogenome), as determined by qPCR. (A) Imaging of mice prior to and (B) ten minutes after intraperitoneal administration of 100 µl luciferin substrate (15mg/ml). Control mice received phosphate-buffered saline instead of pseudovirus. Imaging of control mice was performed (C) prior to and (D) after substrate administration.

All images were taken in the IVIS 100 imaging system using medium binning and 60 s exposure and analyzed with the Living Image 3.0 software. The color scales represent the average radiance given in p/s/cm2/sr.

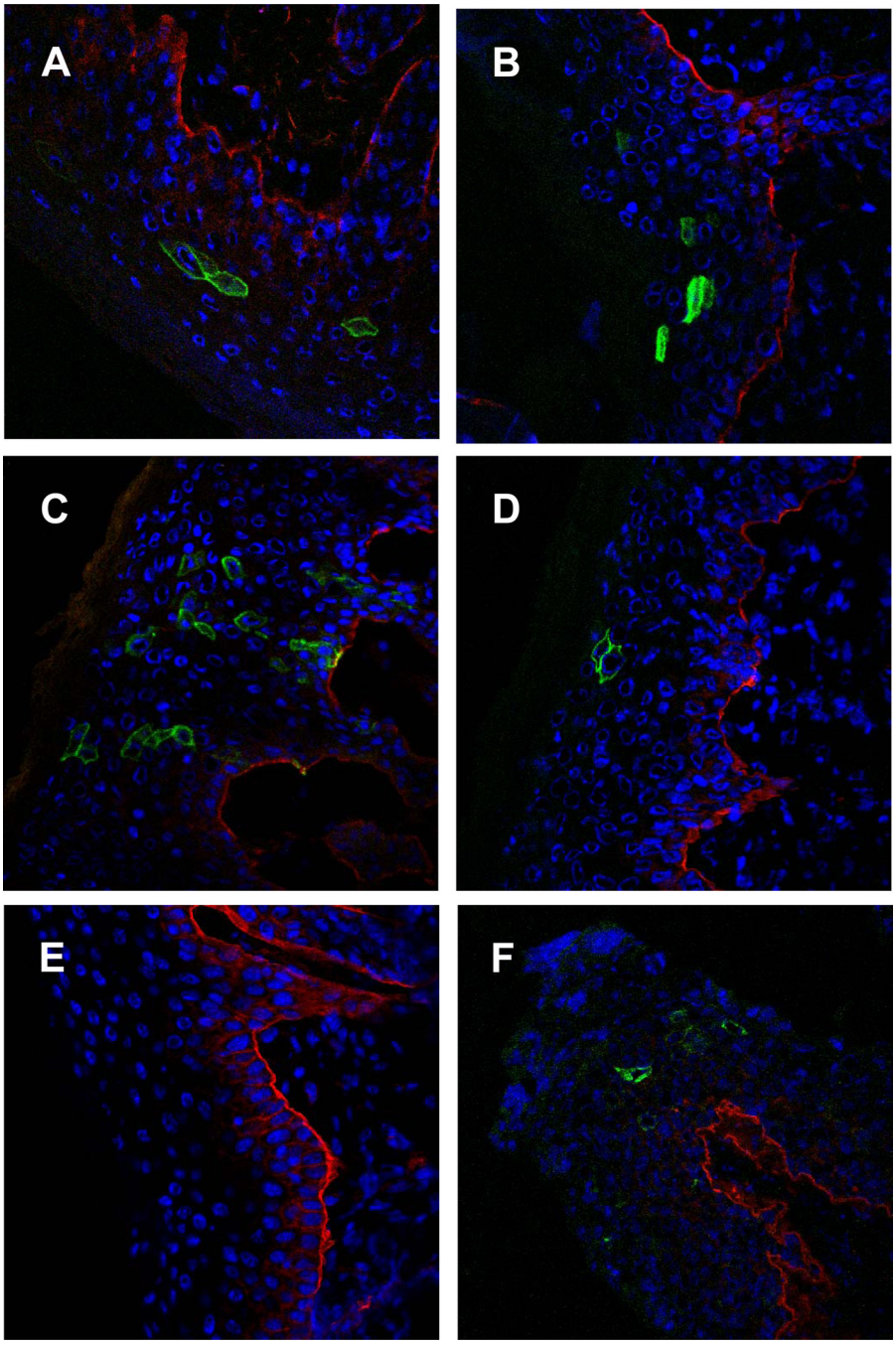


**Fig. 2.**

Cellular distribution of pseudogenome expression for representatives of different human and animal papillomavirus types in the (A–E) skin and in (F) genital tissues, visualized by immunofluorescent staining and confocal microscopy. All pseudovirions encapsidated the reporter gene plasmid pNaMB, which encodes a non-signaling “tailless” human CD4 reporter gene. Detection was performed using an antibody specific for human CD4 followed by Alexa Fluor 488-conjugated secondary antibody (green). To determine the localization of infected cells in relation to the basement membrane, co-staining was performed with an anti-CD49f (integrin alpha 6) phycoerythrin-labeled antibody (red). Skin samples (A–E) were analyzed on day three, genital tissues (F) on day two after infection. The representatives of

human and animal papillomaviruses are as follows: (A) cutaneous HPV 5, (B) mucosal HPV 16, (C, F) mouse papillomavirus and (D) bovine papillomavirus 1. (E) Skin tissues of control mice that were mock-treated with phosphate-buffered saline.

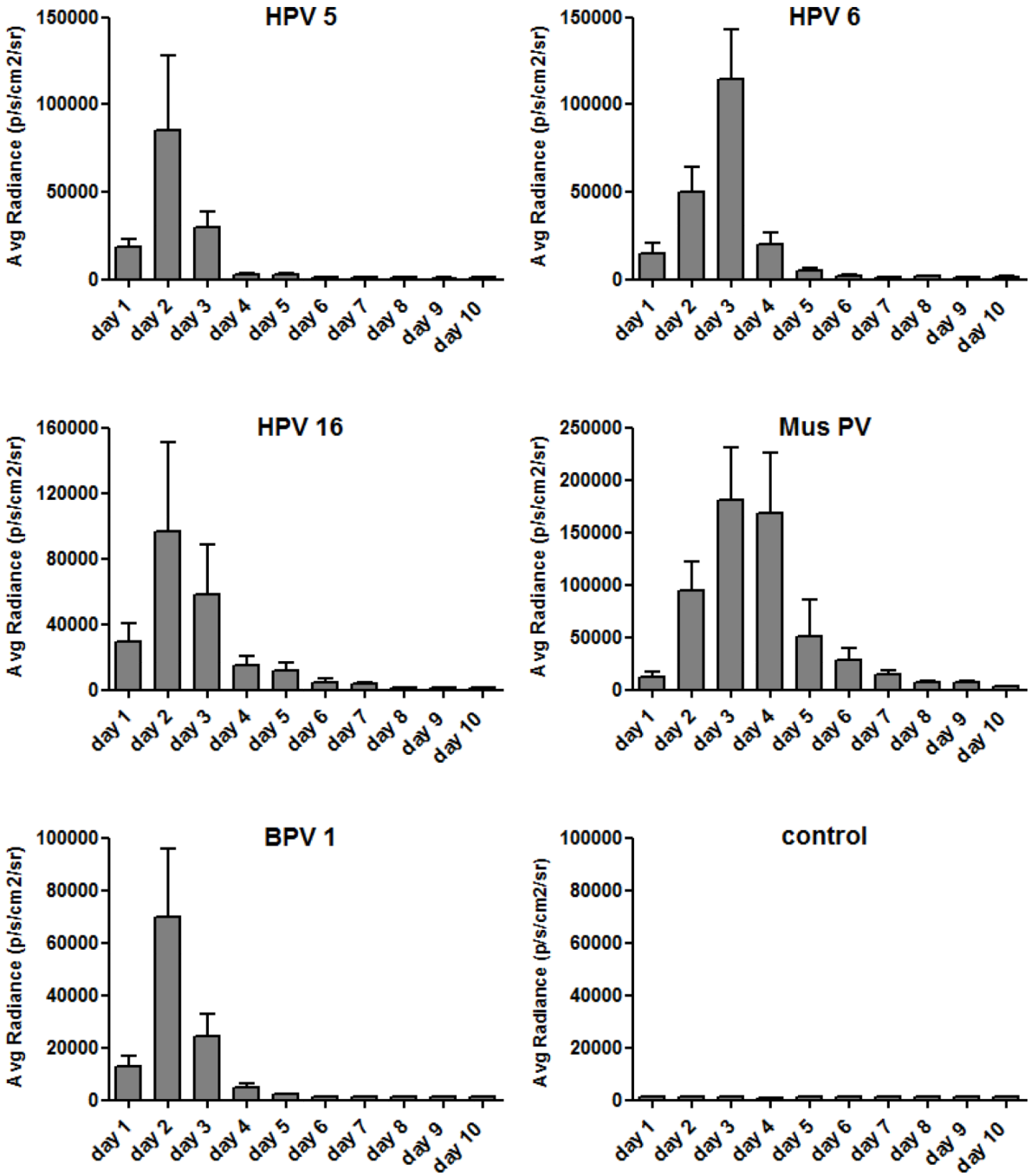


**Fig. 3.**

Dynamics of luciferase expression for representatives of human and animal papillomaviruses. Skin challenge was performed with luciferase-harbouring pseudovirions, corresponding to a total of $1\times10^9$ luciferase pseudogenome copies per inoculation. Readout was performed by *in vivo* imaging analysis daily for ten consecutive days. Control mice received phosphate-buffered saline instead of pseudovirions. The substrate luciferin was administered by intraperitoneal injection. Each experimental group consisted of five animals and results of the average radiance are given in mean p/s/cm2/sr ± standard deviation.

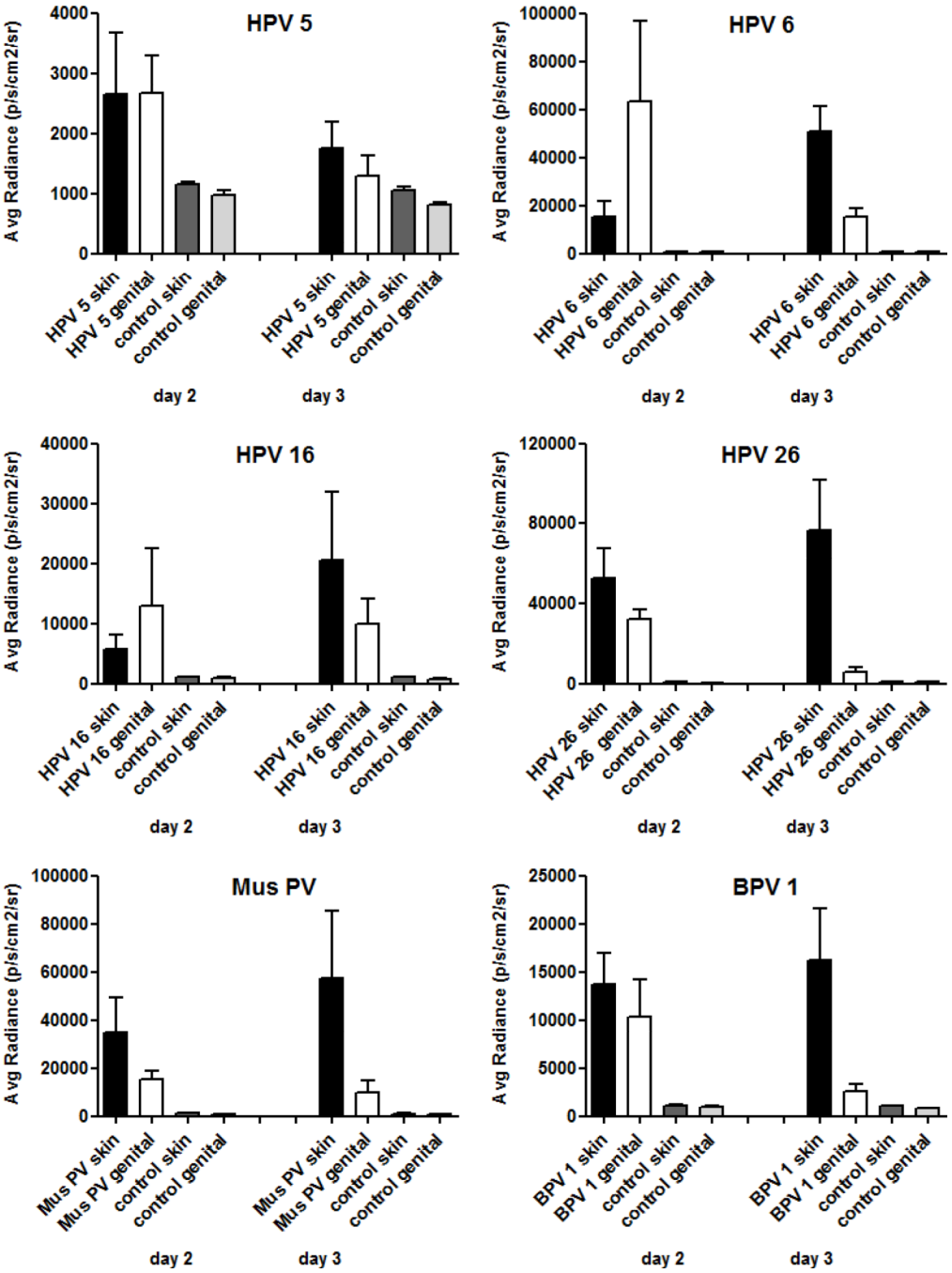


**Fig. 4.**

Comparison of the efficiency of different pseudovirions in infection of murine skin and cervicovaginal tissues. Mice were concomitantly challenged on the skin of the back and in the cervicovaginal tract with pseudovirions carrying an encapsidated luciferase-expressing pseudogenome. The amount for each inoculation corresponded to $1\times10^9$ pseudogenomes, as determined by qPCR. Mice that had been mock-infected with phosphate-buffered saline served as controls. Readout was performed after intraperitoneal administration of the luciferin substrate by *in vivo* imaging analysis on days two and three post infection. Each experimental group consisted of five animals and results of the average radiance are given in mean p/s/cm2/sr ± standard deviation.

## Table 1

Ratio of reporter plasmid copies vs. infectious units or L1 capsids

| pseudovirion types | reporter plasmid copies/ infectious units (mean ± SD) | capsids/1×$10^9$reporter plasmid copies |
|---|---|---|
| HPV 5 | 4811 ± 2249 | 4.70 |
| HPV 6 | 73 ± 21 | 5.51 |
| HPV 8 | 635 ± 777 | 1.35 |
| HPV 16 | 67 ± 26 | 3.78 |
| HPV 18 | 171 ± 16 | 1.47 |
| HPV 26 | 53 ± 34 | 4.41 |
| HPV 44 | 360 ± 13 | 3.36 |
| HPV 45 | 23 ± 33 | 1.33 |
| HPV 51 | 116 ± 28 | 1.14 |
| HPV 58 | 37 ± 62 | 2.5 |
| Mus PV | 28 ± 15 | 2.54 |
| BPV 1 | 174 ± 56 | 1.34 |